Photo catalytic degradation of Indigo carmine in aqueous media using Nano crystalline zirconia by solid state method: synthesis and characterization

Ali H. Alsadoon [(1)],	Alialsoud1987@gmail.com [(1)]University of Babylon, collage of pharmacy,
Baraa Ibrahim Abbas [(2)],	[(2)] Directorate of Education, Al_Karkh the first, Ministry of Education,
Gufran Hade seood, [(3)]	[(3)]Al-Mustaqbal University Collage, dep.of Medical physics
Nada Y.Fairooz [(4)]	[(4)]University of Babylon, collage of science,dep.Of chemistry.

ABSTRACT

The (ZrO2/rGO) Nano composite photo catalytic was made by solid state technique at varied ratios (1:2,2:1,3:4) and calcination at 700 oC for 20 hours in this work. ZrO2/rGO NC was synthesized. FTIR, XRD, UV-Visible, FESEM, Bet, and Bjh were used to examine the prepared powder. The degradation indigo carmine dye (m.f. C16H8N2Na2O8S2) to wavelength of the solution of max(608) nm was projected under high pressure mercury lamp (HPML) OSRAM (125) watts to Nano partials (ZrO2) by solid state method and calcination at temperature 700Co for 20h. The conclusion improved the catalyst's mass, early concentration for (ZrO2/rGO), pH effect, and temperature effect. Microscopy studies revealed that the granules produced for the composite were of a consistent size.

Keywords:	Nanoparticles, zirconium oxide, Photo catalytic, degradation, Solid State method, Nano composite

Introduction

Zirconium oxide is a material of countless technical standing that has decent normal color, has tall strong point, tall hardness, and is considered chemically stable, excellent corrosion, chemical and contagious confrontation [1-2]. zirconium oxide is a extensive-g type p semiconductor that displays abundant oxygen situations on its surface. the tall ion altercation ability and oxidation actions type it valuable in many catalytic methods as catalyst [3] it is also an imperative dielectric existence considered for possible request as a dielectric in transistors in future nano scale electrical employments [4] graphene is an exciting substance. [5] it has a big theoretical specific surface area (2540 m 2 g-1), tall

subjective movement (300,000 cm 2 v - 1 s - 1), [6,7] and has a tall young modulus (~ 1.5 tpa) [8] current conductivity (~4000 wm - 1 k - 1), [9] ophthalmic transmittance (89.7%) and decent electrical conductivity rate courtesy for tenders for example translucent conductive electrodes, [10,11] amongst several other possible applications. graphene has remained calculated experimentally for more than 50 years, [12,13] textile wastewater is among the most pollutants of the environment due to its characteristics such as containing highly oxidant materials as well as highly concentrated due to the constant color, lack of biodegradation and tall PH and T [14]. dye-comprising wastes can impede sunny diffusion in lake, river, or lake water, and thus inhibit photosynthetic biological processes.

moreover, these liquid wastes can contain deadly, carcinogenic, mutagenic or distorted chemicals for numerous microbiological or bodily types [15]. Indigo Carmine, is mostly rummage-sale in the textile business for dye polyester and denim fibers [16]. It is projected that about 40% of the practical dyes continue unstable and are cleared to the waste [17].(IC) is also rummage-sale in various trades due to its high efficacy and is used in foodstuffs, cosmetic trades, as a analytic assistance, as an pointer of reduction in logical interaction, and accurate spots in biology [18]. Several soundings have shown that artificial dyes keep oncogenic and allergenic belongings. However, the dye have been widely recycled in many trades for example paper, fabrics, cosmetics, medicines, and production as a dye due to their informal obtainability [19,20]. Release of these biological toxins the ecology can source grave environmental and human fitness anxieties [21,22].

Experimental

materials and chemicals all the logical mark chemicals counting zirconyl chloride octa hydrate ($ZrOCl_2.8H_2O$) with 96% purity, NaOH and 97% pure H_2SO_4(himedia laboratories pvt. ltd.); graphite precipitate having 93.5% purity (sk carbon ltd.)); HCl (35.4% purity), silver nitrate pure 76%; H_2O_2 pure 86% were obtained from the merck. the deionized water is recycled during the experimental works.

Preparation of ZrO_2 by Solid State methods.

The nanocrystalline zirconia was made utilizing zirconyl chloride ($ZrOCl_28H_2O$) as a precursor in a solid-state process. The effect of Zr/NaOH ratios, calcination and crystallization temperatures, and the involvement of surfactant were studied using a variety of techniques. First, fine powders of $ZrOCl_28H_2O$ and NaOH were ground and blended at room temperature. The mixture was then placed in an autoclave and held at a specific temperature for a specified amount of time. The combination was then washed with deionized water until it was free of Cl ions, and then washed again with ethanol to eliminate any remaining water. Finally, the samples were dried overnight at 383

K. The dried samples were calcined for 20 hours at 700 degrees Celsius[23].

Preparation of graphen e oxide

Graphene oxide was synthesized fromn natural by the modified hummers method. By adding 5g of graphene and 2.5g of sodium nitrate ($NaNO_3$).in 130 ml of sulfuric acid (H_2SO_4).the solution put in ice bath and stirred for half an hours .by the adding of 20 g 0f potassium permanganate with moving at T 20 C^0 and adding distilled water slowly after that added 50 ml of H_2O_2 . the product was eroded by 5% HCL and then with deionized water ,drying at 100C for 2 h[24].

Preparation of reduced graphene oxide (rGO)

Reduced reduced graphene oxide was synthesized by added 80 mg from graphene oxide and add 70 ml distilled water and sonicated for 45 min . after that Mix the solution with cinnamon extract (after mixing 1 gram of cinnamon with 10 ml double distilled water and escalate for 5h at 100c temperature, filter and dry the extract at 100c for 4h). the solution was diverse with the suspension and refluxed the mixture for 35(min) .the yield was wash away with distilled water .dry the yield .[25]

Preparation of Zro_2/rGo Composite

Nano particale Zro_2/ Reduced graphene oxide wes prepared by using precipitation method and solid state method100 mg of synthese ZrO2 was taken in 100 mL of water and inserted into a round flask together with refiuxing for maybe half an hour. 20 mg of able to prepare rGO was displaced in 2 litre of water and provoked for half an hour. To achieve ZrO2 / rGO NC, rGO solution was added dropwise with continuous shaking and mixed was triggered for maybe 24 hours.[26] .

Results And Discussion

X-ray diffraction: The crystal structure is tested by Factors of lattice section and volume, the symmetry of mass is significant for technical, electrical, and optical inquiries nano particular properties. the tests of composite and nano particles were confirmed in the waken of x-ray breakdown structure is called cubique

pattern diffraction. the crystal with gathering room. fig. 1shows diffraction pattern for x-rays for nanoparticles whose composition is distinct the thickness of the crystallite, 2θ (deg) and FWHM(deg). the crystal size is calculated by using the debye-scherer 's equation

D= k λ/ β cos Ɵ

if D is the mean particle size (nm), then k is the length parameters of form 0.9, π is cukα x-ray wavelength, β is cukα linear extension with a

maximum length (radians) of half and the Bragg angle is the same table-1 displays the mean Nano crystalline molecule size samples measured using condition information from the XRD and found to be within the range (18.16-39.64 nm). we notice through the calculations that the crystal size d of the nanomaterial ZrO_2 is much larger than the crystal size of the Composites ZrO_2 /rGO.
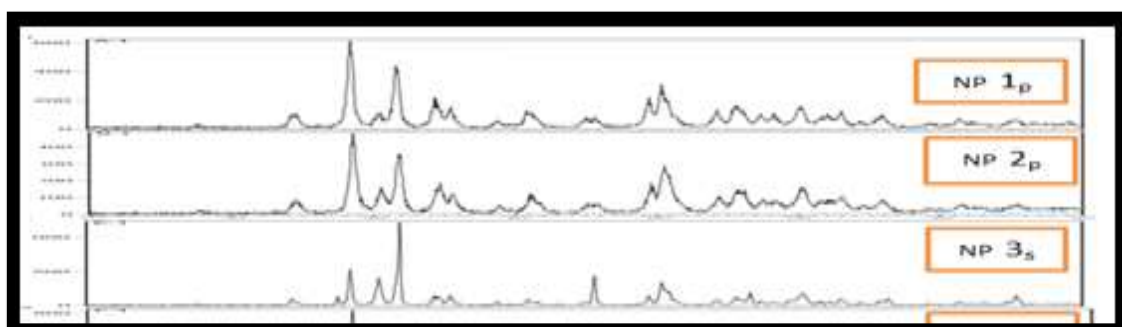

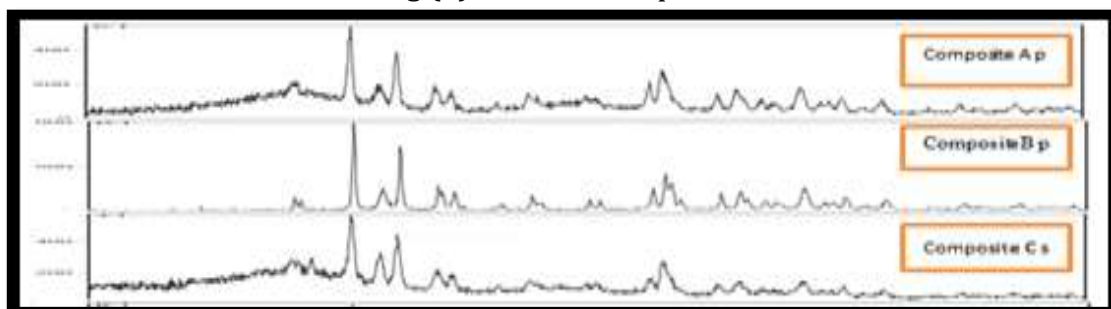Fig (1) XRD of Nano partials

Fig (2) XRD of Composites

3.1 FT-IR analysis FTIR was used to look for functional groups in the synthesized samples. The samples were exposed to infrared radiations ranging from 400 to 4000 cm1 for the analysis. Figure 7 depicts the FTIR spectra of ZrO_2 NM and ZrO_2/rGO NC. Peaks at 3443 cm1 were attributed to hydroxyl stretching, and 1635 cm1 to vibration modes from moisture absorbed on the materials. These two peaks are virtually always present in all FTIR spectra, according to various researchers (Kacurakova et al., 2000; Enferadi & Nejatzadeh-Barandozi, 2012). The distinctive stretching vibration of CH2 is responsible for the large absorption peaks at roughly 2930 cm1. The presence of OH deformations in the C–OH groups causes the

peak at 1387 cm1, while the presence of a sp2 graphite bond causes the peak at 1656 cm1. According to XPS tests, the band at 1060 cm1 belongs to the C–O (epoxy) group, whereas the band at 1100 cm1 belongs to the alkoxy group. 43–45 The absence of peaks in the ZrO_2/rGO spectrum at 1060, 1210, and 1656 cm1 indicates that GO has been reduced to rGO. The Zr–O vibration is responsible for the peak at 470 cm1.These findings could indicate that most oxygen functions in the GO have been eliminated, and ZrO_2/rGO has produced. The intensity of all oxygen-containing moieties in GO has been lowered, indicating a successful and effective reduction of GO to rGO.
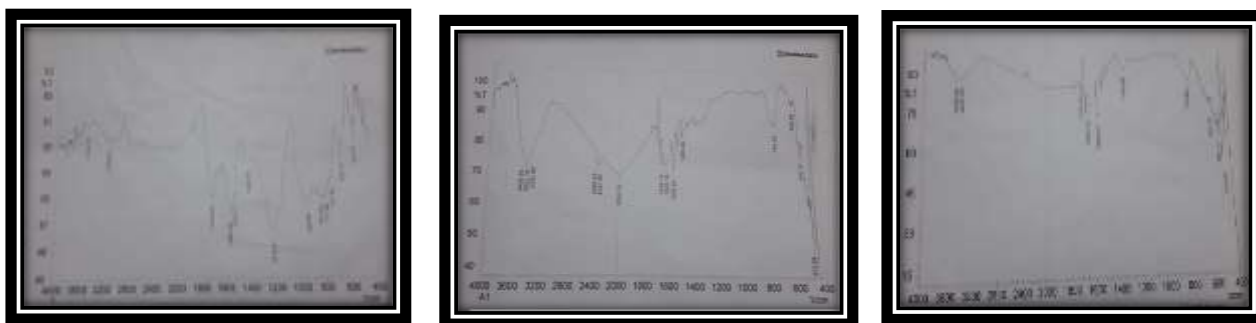
Fig (4) FT-IR of Composites

Electron microscopy (FESEM) field emission scanning offers topographical and kindergarten data at magnifications of 10x to 300,000x, with near limitless depth of view. Compared to conventional electron microscopy scanning (SEM), energy dispersive SEM (FESEM) helps to create slicker, less electrostatically distorted images with a spatial resolution of up to 1 1/2 nanometers-three to six times greater[32]. Grains distribute and aggregate randomly. Due to protein synthesis the particles are isolated as the size of the crystallite increases. The clearly separated porous handful of composite replaced composite are shown at 0.2 having crystalline phase of 63.67 nm The porosity of this trial helps in keeping away from the alteration losses and also the remote particle away from the distortion victims and also the isolated particle improves the transportation properties. Hence, substitution of agglomeration becomes more due of the reduction in crystallite size
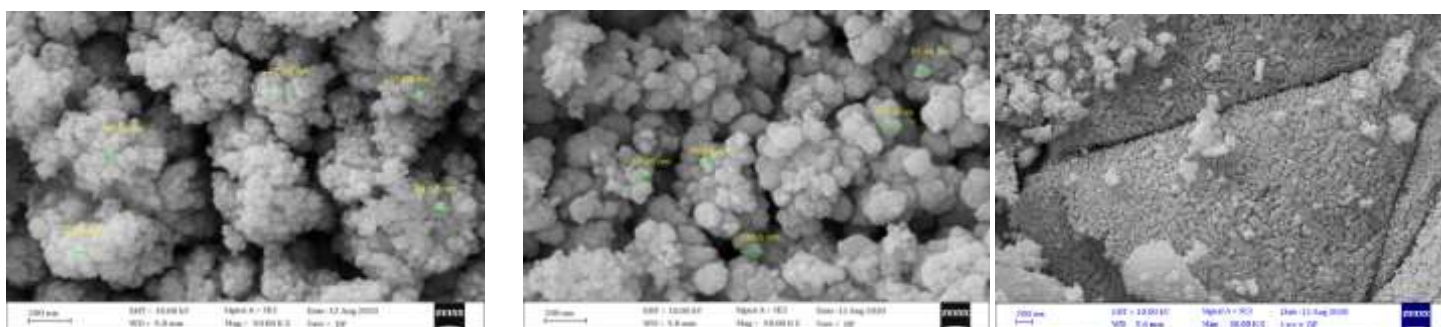

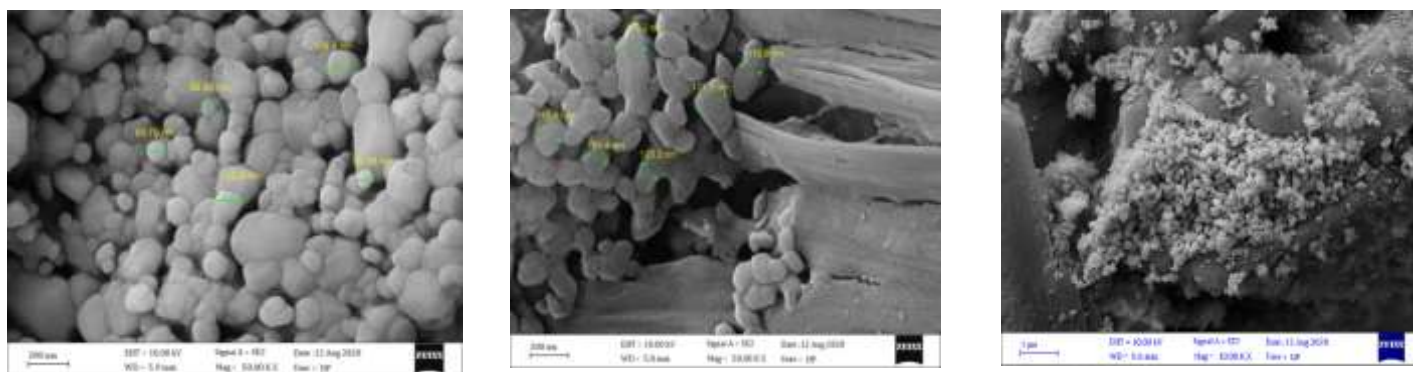**Fig (6) FESEM of Nano partials**

Fig (7) of Nano composites

Brunauer –Emmett-Teller (BET) The surface area on the active site of the surface catalyst was determined according to the BET process, depending on the adsorption and desorption of nitrogen gas. Figures(9)and(10) demonstrate the NP nanoparticles BET plots and the A and B composites. The approximate NP surface area measured using the BET-equation multipoint is 16.072 m2/g and the BET single point is 18.7722 m2/ g. Assuming the particles have a solid, spherical form with a smooth surface, and the single point BET is11,3879 m2/g and the specific area of composite A calculated using the single point BET is24,1940 m2/g and the specific area of B calculated using the multipoint BET-equation is 48,249 m2/g.
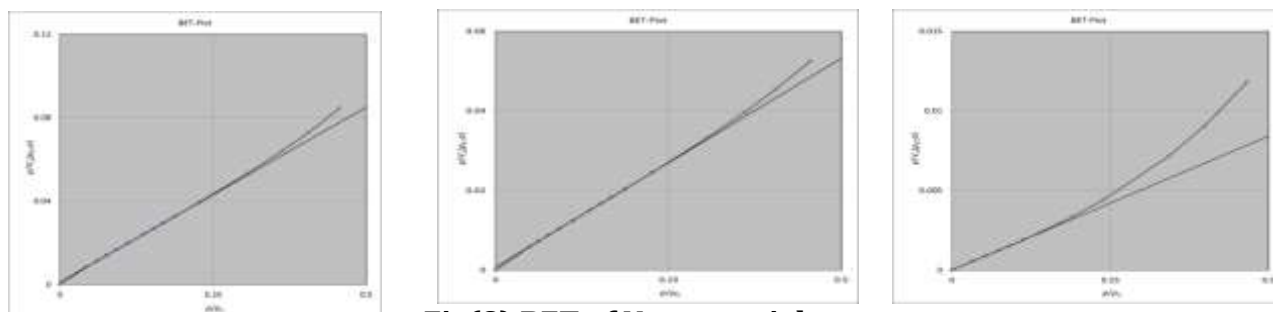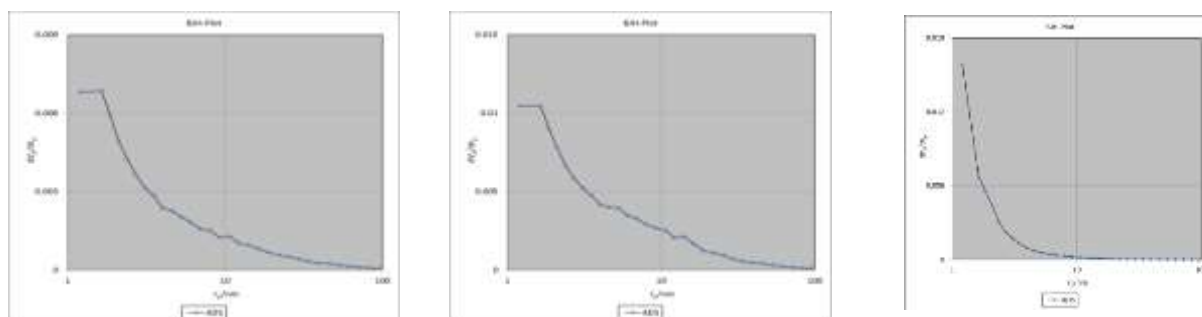

Fig(8) BET of Nano partials
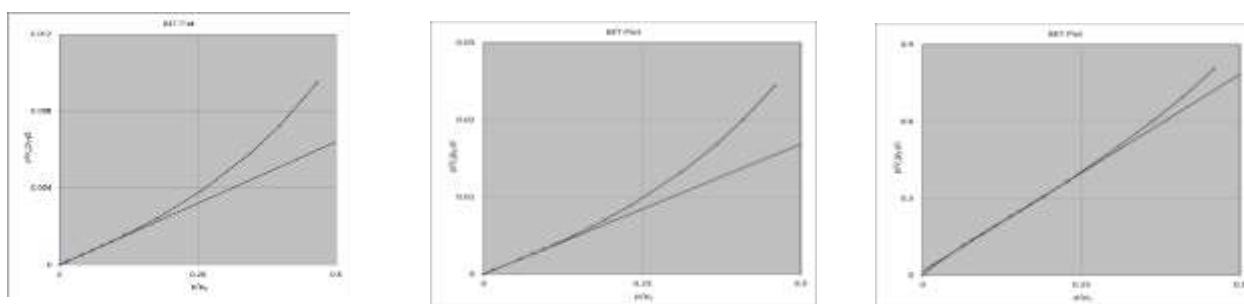
Fig (10) BET of Nano composites

Barret-Joyner-Halenda (BJH) The method developed by (BJH) is most commonly used to assess the quantities, size and distribution of the pore in the adsorbent. Figure(11)and(12) indicates — surface area of prepared desorption NP material at 16,427 m2 / g,15,942 m2 / g and prepared adsorption and desorption NP material at 17,083 m2 / g, 18,267 m2 / g and surface area of prepared adsorption and desorption composite materials (A) at 102,030 m2 / g, 112,616 m2 / g and composite material B at 48,446 m2 / g, 45,320 m2 / g.
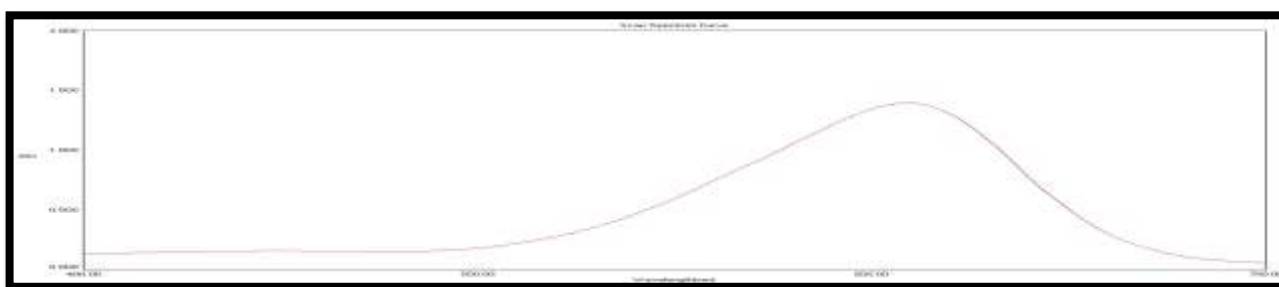

Fig (11) BJH of Nano partials
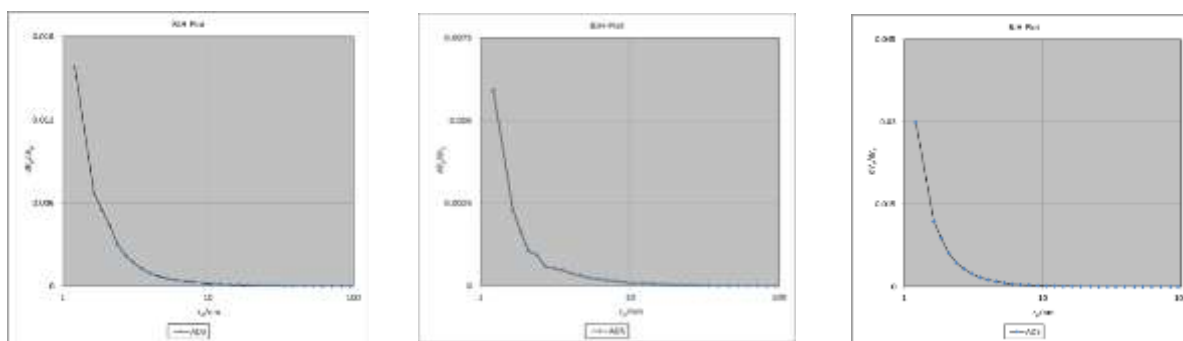
Fig (12) BJH of Nano composites

UV-Vis. Spectrophotometer T80 UV-Vis Double beam PG spectrophotometer is used for the study of indigo carmine dye degrad ation behavior over composite[33]. Then assess λmax for indigo carmine dye. It was found that λmax = 608 nm at a concentration of 60ppm

Fig (13) UV-Visible of Indigo carmine dye

Effect of Catalyst Mass Distinctive experiments in this study were conducted using standardized measures (0.01, 0.1, 0.15, 0.2, 0.25, and 0.3) grams respectively. At all tests the indigo carminedye concentration was held constant (10 ppm). Therefore, all other parameters remained constant: medium pressure mercury lamp (MPML) irradiation 125 w air simmer speed 10 cm3 / min inter to photocatalytic cell, pH = 7 and light force 8.67 mW / cm2 at height 7 cm at 25 0C [34].
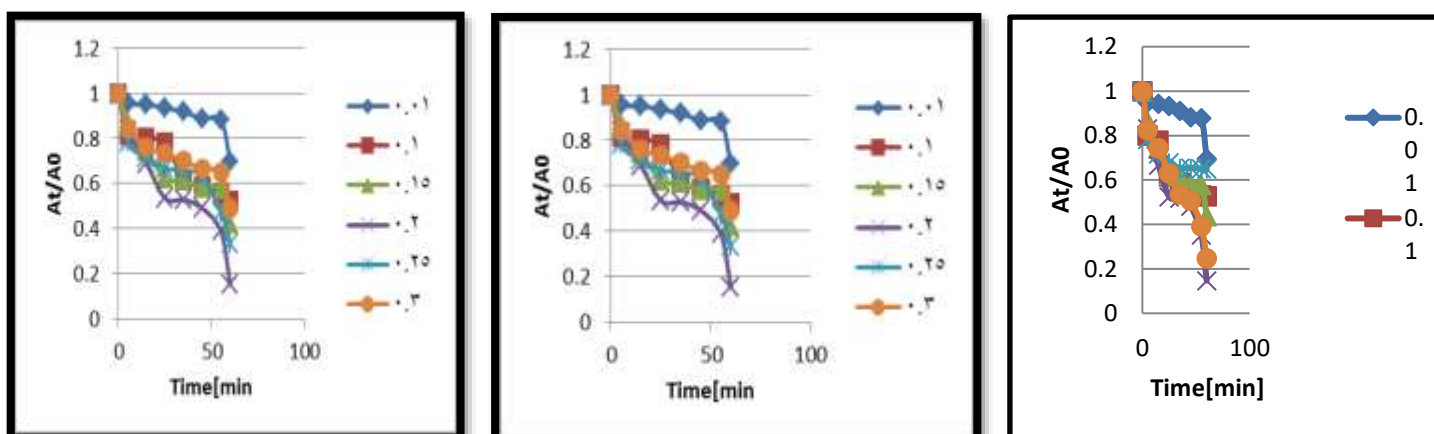
Fig(14):Effect of the catalyst mass on photo degredation

Effect of Initial Concentration of Indigo Carmine Dye In this part different concentrations of indigo carmine dye were taken in various initial concentrations of substratum (5, 10, 30, 50 and 70) ppm with 0.3 g of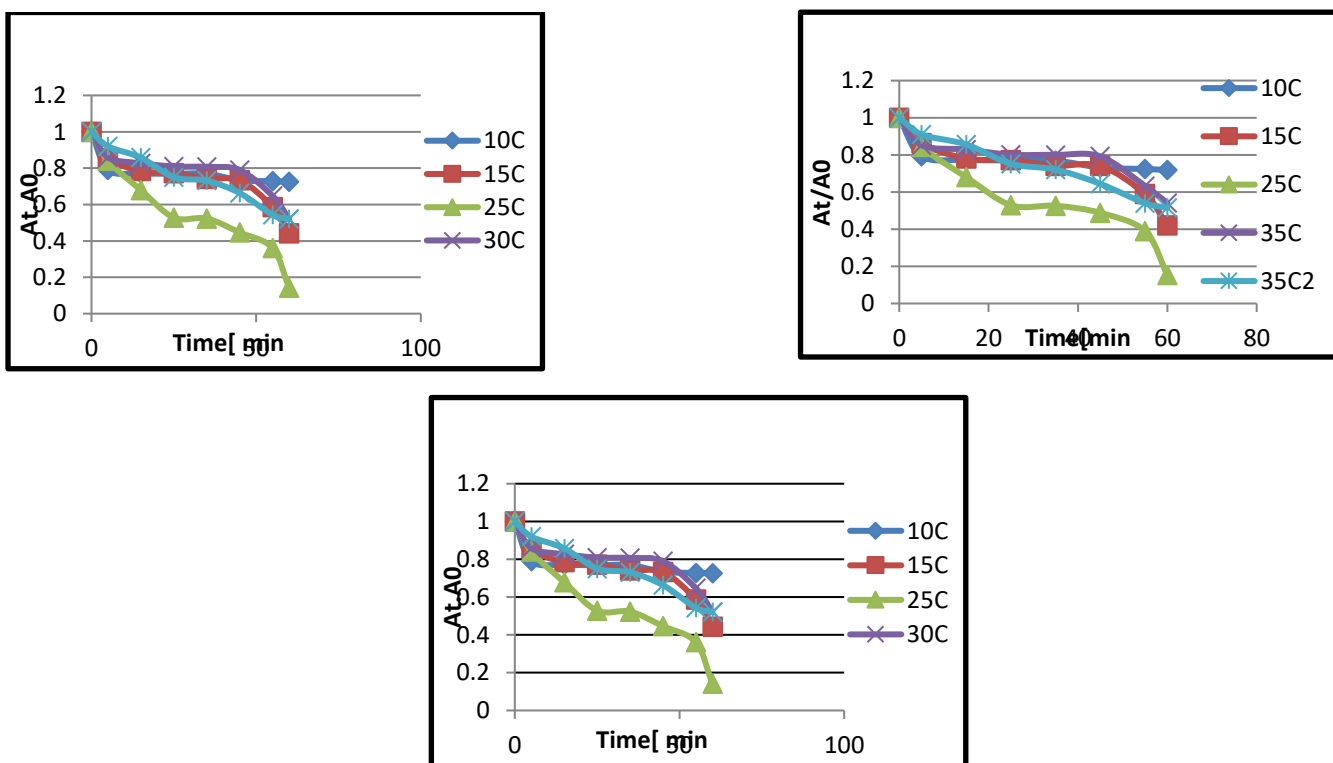 composite In addition, all other conditions remained constant: medium pressure mercury lamp (MPML) 125 watts irradiation, air simmer speed 10 cm3 / min inter to photocatalytic cell, pH = 7 and light force 8.67 mW / cm2 on photocatalytic cells[36].
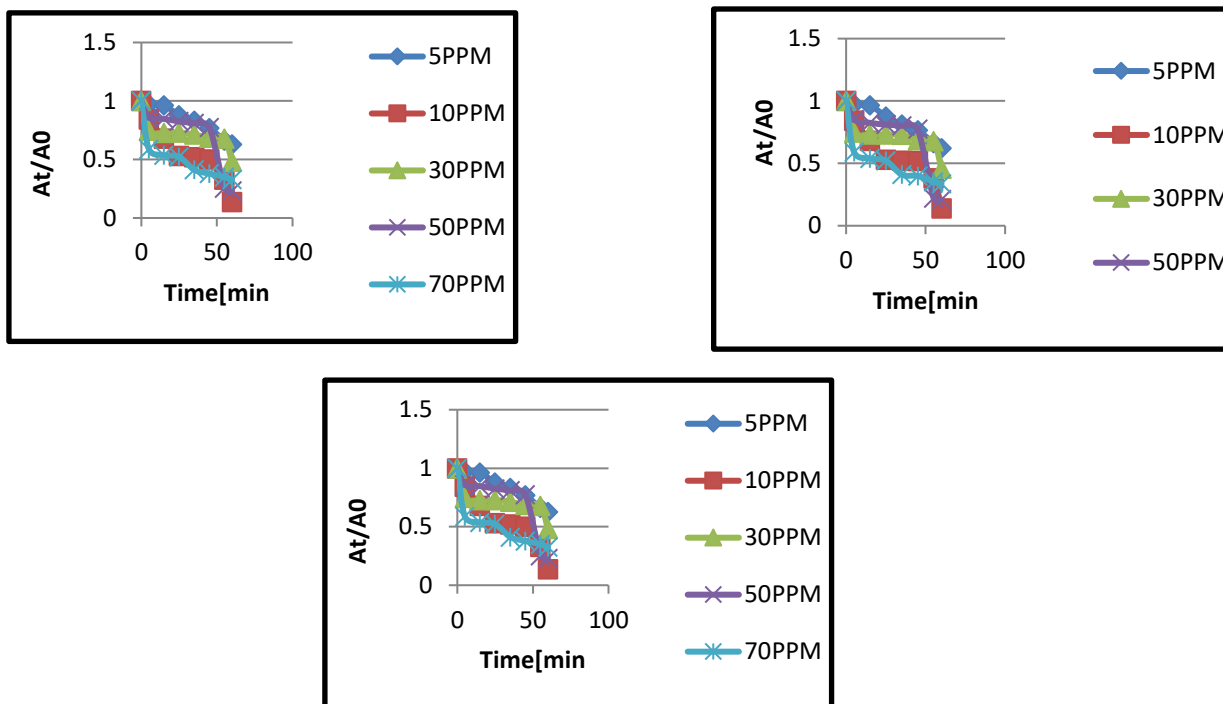
Fig(15):Effect of the concentration of indigo carmine dye

Effect of Temperature The effect of temperature on the process of photocatalytic degradation was achieved with series of experiments at different temperatures (10C, 15C, 25C, 30C, and 35C). At optimum condition .with concetration of composite 0.3 g all the rest conditions were kept constant: The concentration ofindigo carmine dye 10 ppmand, irradiation of medium pressure mercury lamp (MPML) 125 w, air simmer speed 10 cm3 / min inter to photocatalytic cell, pH = 7, light intensity 8.67 mW / cm2 and height 7 cm[35].

Fig(16): The change of At/A0 with time at dissimilar temperature of composite A&B on photo Degradation

Effect of pH The pH effect of indigo carmine dye solution on photocatalytic degradation process was achieved by conducting series of tests at different pH (3, 5 , 7, 9, and 11) at optimum catalyst mass 0.3 gram composite level. Furthermore, all the remaining conditions remained constant: indigo carmine dye concentration 10 ppm, medium pressure mercury lamp (MPML) irradiation 125 w, air simmer speed 10 cm3 / min inter to photocatalytic cell at 25 0C [36]
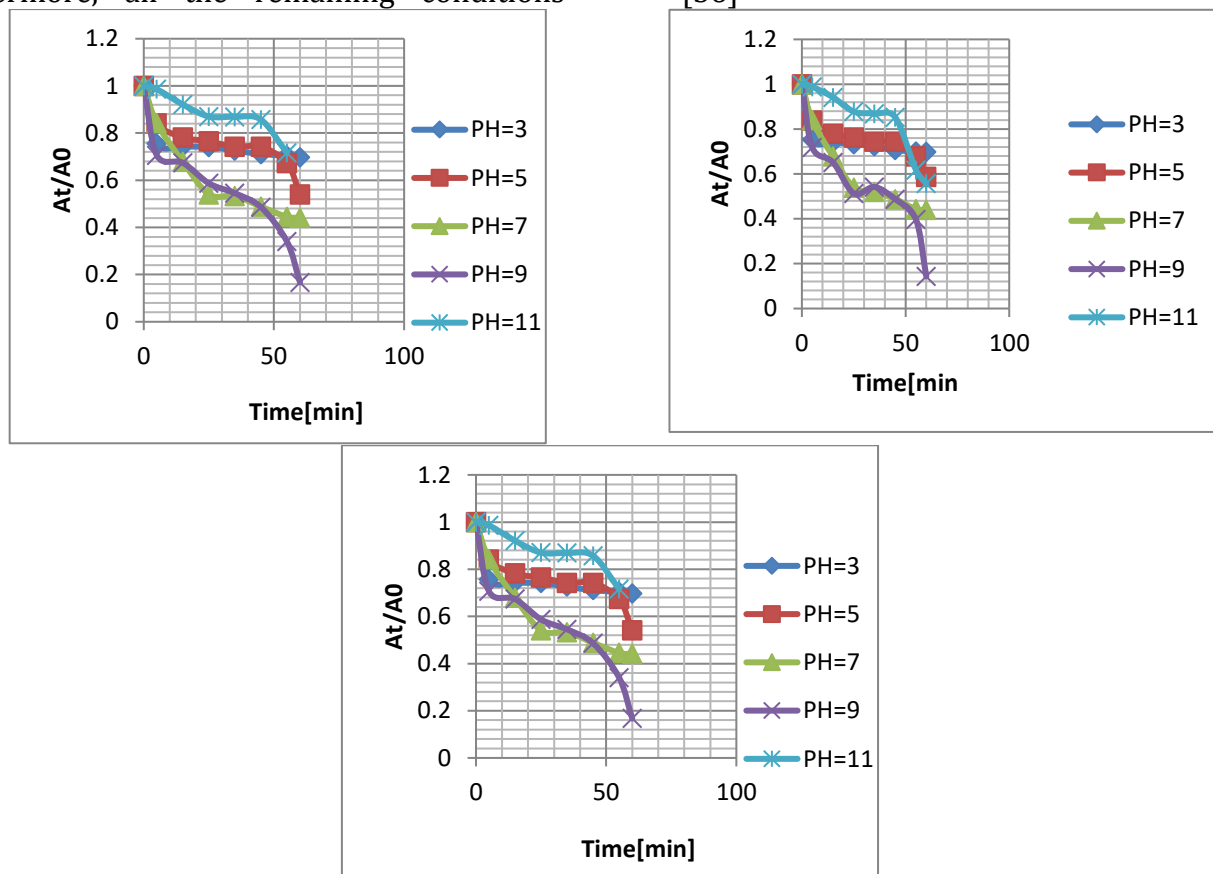
Fig(17): Effect of PH of dye solution composite A,B and C on photo degradation

4.Conclusion

The present work can be see that the ZrO_2 nanoparticles were successfully making using the solid state technique Using an environmentally friendly and environmentally friendly Path An existing and simple approach to rGO prepare using Cinnamon extract. we prepare ZrO_2/rGO NC during a facile rainfall technique at area temperature. The foundation of ZrO_2/rGO was inveterate by some description methods The description marks presented that the produced ZrO_2/rGO nano composite were shapeless in environment and exhibition a monoclinic chapter of ZrO_2 in composite with sphere-shaped morphology exhibiting fine band gap related to plain ZrO_2 nanoparticles .The photo catalytic investigational marks exposed that ZrO_2/rGO NC degrades indigo carmine dyes in the equal response complaint by 85% at best disorder of 0.3 g (composite), concentration of dye 10 ppm,and temperature equael to25ºC, pH equeal to 7 having radioactivity at time 60 min. depend on our soundings and got investigational marks we determined that produced ZrO_2/rGO is an outstanding photo catalyst.

References

1. Hirvonen, R. Nowak, Y. Yamamoto, T. Sekino, K. Niihara, "Fabrication, structure mechanical and thermal properties of zirconia-based ceramic nano composites," J.Eur Ceram. Soc., vol. 26, pp. 1497-1505, 2006.
2. J.C. Ray, D. Park, W Ahn, "Chemical synthesis of stabilized nanocrystaline zirconia powders," J. Ind. Eng. Chem, vol. 12, no, 1, pp.142-148, 2006.

3. J. L. Gole, S. M. Prokes, J. D. Stout, O. J. Yang R. Glembocki, "Unique properties of selectively formed zirconia nano structures," Adv. Mater. Vol. 18, pp.644-649, 2006.

4. G. Dutta, K. P. S. S. Hembram, G. M . Rao, U. V. Waghmare, "Effects of O vacancies and C doping on dielectric properties of ZrO2: A first-principles study," , .pp. 202904, 2006. Appl. Phys.Lett., vol89

5. K. Geim , K. S. Novoselov , Nat. Mater. 2007 , 6 , 183] . 5[P. Kim K. I. Bolotin , K. J. Sikes , Z. Jiang , M. Klima , G. Fudenberg , J. Hone] ,

6. H. L. Stormer , Solid State Commun. 2008 , 146 , 351.

7. S. V. Morozov , K. S. Novoselov , M. I. Katsnelson , F. Schedin , D. C] .Elias , J. A. Jaszczak , A. K. Geim , Phys. Rev. Lett. 2008 , 100 , 016602.

8. Lee , X. D. Wei , J. W. Kysar , J. Hone , Science 2008 , 321 , 385

9. A. Balandin , S. Ghosh , W. Z. Bao , I. Calizo , D. Teweldebrhan] , F. Miao , C. N. Lau , Nano Lett. 2008 , 8 , 902.

10. W. Cai , Y. Zhu , X. Li , R. D. Piner , R. S. Ruoff , Appl. Phys. Lett. 2009] , 123115,95.

11. X. Li , Y. Zhu , W. Cai , M. Borysiak , B. Han , D. Chen , R. D. Piner] ,

12. L. Colombo , R. S. Ruoff , Nano Lett. 2009 , 9 , 4359.

13. H. P. Boehm , A. Clauss , G. O. Fischer , U. Hofmann , Z. Anorg. Allg] .Chem. 1962 , 316 , 119.

14. X. K. Lu , H. Huang , N. Nemchuk , R. S. Ruoff , Appl. Phys. Lett 193,75,1999

15. O'neill, F.R. Hawkes, D.L. Hawkes, N.D. Lourenco, H.M. Pinheiro, W. DeleeColour in textile effluents—sources, measurement, discharge contents and simulation: a review, J. Chem. Technol. Biotechnol. 74 (1999) 1009–1018.

16. Willcock, M. Brewster, W. Tincher, Using electrochemical technology to treat textile wastewater: three case studies, Am. Dyestuff Rep. (1992) 15–22.

17. Gutiérrez-Segura, M. Solache-Ríos, A. Colín-Cruz, Sorption of indigo carmine bya Fe-zeolitic tuff and carbonaceous material from pyrolyzed sewage sludge, J.

18. Hazard. Mater. 170 (2009) 1227–1235.

19. B. Manu, Physico-chemical treatment of indigo dye wastewater, Color. Technol . 202-197(2007)123

20. U.R. Lakshmi, V.C. Srivastava, I.D. Mall, D.H. Lataye, Rice husk ash as an effectiveadsorbent: evaluation of adsorptive characteristics for Indigo Carmine dye, J.Environ. Manage. 90 (2009) 710–720..

21. S. Allahveran, A. Mehrizad, J. Mol. Liq. 225, 339 (2016)

22. E.B. Yazdani, A. Mehrizad, J. Mol. Liq. 255, 102 (2018)

23. S. Rani, M. Aggarwal, M. Kumar, S. Sharma, D. Kumar, Water Sci. 30, 51 (2016

24. Liu, S. Deng, A. Maimaiti, B. Wang, J. Huang, Y. Wang, G. Yu, J. Colloid Interface Sci. 511 (2018). 277

25. Roberts M. J., Everson R. C. , Neomagus H.W.J.P., Van Niekerk D. , Mathews J. P., Branken D. J. (2015) Influence of maceral composition on the structure, properties and behaviour of chars derived from South African coals. Fuel 142: 9–20

26. Hummers and R. E. Offeman, J. Am. Chem. Soc., 1958, 80, 1339. W. S

27. S. Gurunathan, J. W. Han, V. Eppakayala and J. Kim, Colloids Surf., B, 2013, 102, 772

28. D. Suresh, Udayabhanu, H. Nagabhushana and S. C. Sharma, Mat. Lett., 2015, 142, 4.

29. Y. Sugimoto, P. Pou, M. Abe, P. Jelinek, R. Perez, S. Morita and O. Custance, Nature, 446, 64 (2007)

30. K. Chang, S. Cheng, Y. Chen, H. Huang and J. Liou, J. Microbiol. Immunol. Infect., 46, 405 (2013).

31. P. West, "Atomic Force Microscopy", 1st edi., United States by Oxford University Press Inc., New York, 2010.

32. M.J. Doktycz, C.J. Sullivan, P.R. Hoyt, D.A. Pelletier, S. Wu and D.P. Allison, Ultramicroscopy, 97, 209 (2003)

33. Y. Sugimoto, P. Pou, M. Abe, P. Jelinek, R. Perez, S. Morita and O. Custance, Nature, 446, 64 (2007)

34. Patterson, A., The Scherrer formula for X-ray particle size determination. Physical review 1939, 56 (10), 978.

35. Monshi, A.; Foroughi, M. R.; Monshi, M. R., Modified Scherrer equation to estimate more accurately nano-crystallite size using XRD. World Journal of Nano Science and Engineering 2012, 2 (3), 154-160.

36. Einaga, H.; Mochiduki, K.; Teraoka, Y., Photocatalytic oxidation processes for toluene oxidation over TiO2 catalysts. Catalysts 2013, 3 (1), 219-231.

37. Rusmidah, A.; Abu, B.; Teck, L., Zn/ZnO/TiO2 and Al/Al2O3/TiO2 photocatalysts for the degradation of cypermethrin. Modern Applied Science 2010, 4 (1), 59-67.

38. Lydakis-Simantiris, N.; Riga, D.; Katsivela, E.; Mantzavinos, D.; Xekoukoulotakis, N. P., Disinfection of spring wat